JOURNAL OF GEOPHYSICAL RESEARCH, VOL. 103, NO. A9, PAGES 20,449-20,458, SEPTEMBER 1, 1998

Cyclotron amplification of whistler waves by electron beams in an inhomogeneous magnetic field

Y. Hobara,[1] V. Y. Trakhtengerts, and A. G. Demekhov
Institute of Applied Physics, Nizhniy Novgorod, Russia

M. Hayakawa
Department of Electronic Engineering, The University of Electro-Communications, Tokyo, Japan

Abstract. Cyclotron wave-particle interactions in the case of well-organized distributions of energetic electrons under an inhomogeneous magnetic field are studied. Step-like and δ function distributions over the field-aligned velocity are considered. The one-hop amplification of whistler waves is calculated by simple analytical solution and numerical computation based on strict approach. The strict consideration, taking into account third-order expansion of the spatial dependence of the electron phase with respect to the wave, reveals some new important features of the one-hop amplification Γ as a function of frequency and electron beam parameters. The main result is that Γ exhibits a quasi-periodic structure as a function of wave frequency or characteristic electron parallel velocity, remaining always positive in the case of the step-like distribution but being sign alternative for δ-function. Dependence of Γ on the parameters of energetic electrons such as their total energy, characteristic parallel velocity, position of the injection point in relation to the equator, and dispersion in parallel velocity is discussed.

1. Introduction

The cyclotron interaction of whistler waves with well-organized beams of energetic electrons in the inhomogeneous magnetic field attracts a lot of interest in connection with some important problems of magnetospheric physics. The first problem is triggered ELF/VLF emissions; quasi-monochromatic whistler signals are excited by beams of energetic electrons produced in the process of interaction between a monochromatic whistler wave packet and electrons in the radiation belt [e.g., *Karpman et al.*, 1974; *Nunn*, 1974]. The problem closely associated with this problem is chorus generation when whistler signals with discrete frequency spectrum are excited under the natural conditions of the magnetosphere [*Hattori et al.*, 1989, 1991]. Another problem that demands the consideration of interaction between waves and a well-organized beam of electrons in an inhomogeneous magnetic field is wave generation in the auroral zone, where a strong acceleration of charged particles by a field-aligned electric field takes place. By well-organized beams we mean the groups of energetic electrons with small velocity dispersion, where the hydrodynamic stage of the instability is realized in the case of homogeneous magnetic field. Examples of such beams are energetic electrons with velocity distribution along the magnetic field as a step-like function or Dirac function. Formation of such distribution functions in the magnetosphere is quite real (indeed, the step-like distribution is formed by the quasi-linear relaxation of beam plasma and cyclotron instabilities [*Ivanov*, 1977; *Trakhtengerts et al.*, 1986]), and calculations performed in the framework of quasi-linear theory show a very large increase of amplification during the formation of a step [*Trakhtengerts et al.*, 1996]. The real situation with the δ distribution function is beam formation by cyclotron interaction of a quasi-monochromatic whistler wave packet with radiation belt electrons [*Karpman et al.*, 1974; *Nunn*, 1974].

In this paper we shall analyze the effects of cyclotron instability in the presence of such beams in an inhomogeneous magnetic field. Some new effects are found to be important, and they determine the cyclotron instability development. The hydrodynamic stage of the instability is modified in the inhomogeneous magnetic field, and certain new specific wave generation regimes can take place [*Trakhtengerts*, 1995]. The most important effect in the inhomogeneous magnetic field is the mismatching of the cyclotron resonance condition,

$$\omega - \omega_H = k v_{\|} \qquad (1)$$

[1] Now at Department of Electronic Engineering, The University of Electro-Communications, Tokyo, Japan.

Paper number 98JA01746.
0148-0227/98/98JA-01746$09.00

where ω and k are frequency and wave vector of a whistler wave ($k \parallel \vec{H}$, $\vec{H}$ is the geomagnetic field), ω_H is the electron gyrofrequency, and $v_\parallel$ is the electron velocity component along the magnetic field. In (1), ω_H, k and $v_\parallel$ depend on the coordinate z along $\vec{H}$. When ω is fixed, the resonance condition (1) is fulfilled in the linear stage of the instability only at one point. Under these conditions the second-order cyclotron resonance [*Helliwell*, 1967; *Nunn*, 1974; *Villalón and Burke*, 1997] can be important when the frequency of the whistler wave packet depends on z and t, and this dependence compensates the mismatching caused by the magnetic field inhomogeneity. The mismatch from the resonance condition (1) can be compensated also for a wave with fixed frequency by suitable gradients of the magnetic field and cold plasma density if the electron velocity changes under the action of the wave field are taken into account; such compensation can occur for a small group of particles and depends on the whistler wave amplitude, its contribution to the cyclotron resonant interactions between particles and whistler waves being yet to be determined [*Erokhin et al.*, 1996]. In this paper we analyze the cyclotron instability of a well-organized beam in the regime of stationary amplification [*Trakhtengerts et al.*, 1996], when the density of the beam is relatively small and second-order cyclotron resonance effects are absent. This problem was discussed earlier for a step-like distribution function [*Trakhtengerts et al.*, 1996; *Bespalov and Trakhtengerts*, 1986; *Nunn and Sazhin*, 1991; *Villalón and Burke*, 1997]. Here we discuss some new peculiarities of this problem. Together with the step-like distribution function we consider a distribution with δ function over $v_\parallel$. To be close to the realistic situation, we consider the injection of a beam at an arbitrary point along the magnetic flux tube and take into account a dispersion over $v_\parallel$.

2. Formulation of the Problem (Simplified Consideration)

The problem of whistler wave amplification in an inhomogeneous magnetic field in its full form is rather difficult and has no general analytical solution. Below we shall consider the case when a beam density is sufficiently small and change of phase between wave and particle is determined by mismatching of the cyclotron resonance condition (1) along the particle trajectory (along z) in an inhomogeneous magnetic field. In this case the one-hop amplification $\Gamma = \ln A_f/A_0$ (A_f and A_0 are the final ($z = l$) and initial ($z = -l$) whistler wave amplitudes, and $z = \pm l$ are the ends of the magnetic flux tube) can be presented in the form [*Trakhtengerts et al.*, 1996]

$$\Gamma = \frac{\pi^2 e^2}{cm^2} \int_{W_{RL}}^{\infty} \int_0^{\frac{W-W_{RL}}{H_L}} \left[\frac{I_\perp H^2 dW dI_\perp}{N_w (W - I_\perp H)} \left(\frac{\partial F_0}{\partial W} + \frac{e}{mc\omega} \frac{\partial F_0}{\partial I_\perp} \right) \mathcal{I} \right]_{z_{st}(W, I_\perp, \omega)} \quad (2)$$

where

$$\mathcal{I} = \left| \int_{-l}^{l} dz \exp\left(i \int_0^z \frac{\Delta}{v_\parallel} dz' \right) \right|^2 \quad (3)$$

and $\Delta = \omega - \omega_H - k v_\parallel$. The limit of integration in (2) is determined from the condition that the lowest resonant energy $W_{RL} = m v_{RL}/2$ is achieved at the eqator ($v_{RL} = (\omega_{HL} - \omega)/k_L$, where subscript L refers to any value at the equatorial plane). Further, m is the electron mass, e is magnitude of electron charge, and c is the light velocity. Like *Trakhtengerts et al.* [1996], we have used in (2) the variables of energy W and the first adiabatic invariant $I_\perp$,

$$W = \frac{m}{2}(v_\parallel^2 + v_\perp^2), \qquad I_\perp = \frac{m}{2}\frac{v_\perp^2}{H}, \qquad v_\parallel = -(W - I_\perp H)^{1/2} \left(\frac{2}{m}\right)^{1/2} \quad (4)$$

N_w is the whistler wave refractive index, H is the magnetic field amplitude, and the stationary point z_{st} is determined from the equality $\Delta = 0$. We shall consider the case of the stationary particle injection for two types of distribution functions F_0 of energetic electrons. The first one, a step-like distribution function, appears under the cyclotron interaction of smooth distributions with noise-like whistler emissions [*Trakhtengerts et al.*, 1986, 1996; *Nunn and Sazhin*, 1991] and can be written as

$$F_{\text{step}} = b_{\text{step}} \cdot \Theta(W_* - W + I_\perp H_1), \qquad \Theta(x) = \begin{cases} 1, & x > 0 \\ 0, & x \le 0 \end{cases} \quad (5)$$

where the step-like feature corresponds to the boundary of the resonant and nonresonant particles in the velocity space satisfying the equalities $v_\parallel = v_* = (2W_*/m)^{1/2}$ at the injection point. The step height b_{step} can be determined from the normalization condition [*Trakhtengerts et al.*, 1996],

$$b_{\text{step}} \approx n_h \left(\frac{m}{2\pi W_0}\right)^{3/2} \frac{I_\perp H_1}{W_0} \exp\left(-\frac{W}{W_0}\right) \quad (6)$$

where $W_0 \equiv m v_0^2/2$ is the characteristic energy and n_h is the beam density. The value H_1 is equal to the magnetic field amplitude in an injection point; when H_1 is equal to the equatorial value H_L, we have the case considered earlier by *Trakhtengerts et al.* [1986, 1996] and *Villalón and Burke* [1997]. The second type of a distribution function as δ function over $v_\parallel$ is important for triggered ELF/VLF emissions and appears under cyclotron interaction of electrons with a packet of quasi-monochromatic whistler waves. We take this distribution in the following form:

$$F_\delta = b_\delta \cdot \delta(W_* - W + I_\perp H_1) \quad (7)$$

where

$$b_\delta = \frac{m^{3/2} n_h W_*^{1/2}}{\sqrt{2}\pi W_0} \exp\left(-\frac{I_\perp H_1}{W_0}\right) \quad (8)$$

The function (6) corresponds to the stationary injection from the point z_1, where $H_1 = H(z_1)$. Substituting (5)-(6) into (2) and using new variables,

$$X = I_\perp H_1 \qquad \text{and} \qquad Y = W - X \tag{9}$$

we get the following amplification for the step:

$$\begin{aligned}\Gamma_{\text{step}} &= \left(\frac{\pi}{8mW_0^5}\right)^{1/2} \frac{e^2 n_h}{cN_w}\left(\frac{\omega_{H1}}{\omega}-1\right)\int_0^\infty \delta(W_* - Y) \\ &\times \int_{X_{\min}}^\infty \left(\frac{H_{st}}{H_1}\right)^2 \frac{X^2}{Y + X\left(1-\frac{H_{st}}{H_1}\right)} \\ &\times \exp\left(-\frac{X+Y}{W_0}\right) \mathcal{I}\, dX\, dY \\ &= \frac{\pi^{1/2} e^2 n_h v_0 \exp(-v_*^2/v_0^2)}{2cmN_w}\left(\frac{\omega_{H1}}{\omega}-1\right) \\ &\times \int_{x_{\min}}^\infty \left(\frac{H_{st}}{H_1}\right)^2 \frac{x^2 \exp(-x) dx}{v_{\parallel st}^2}\, \mathcal{I}\end{aligned} \tag{10}$$

where $H_{st} = H(z_{st})$, $x = X/W_0$, $x_{\min}$ is determined below (equation (14)), and

$$v_{\parallel st} = \sqrt{v_*^2 + x v_0^2\left(1 - \frac{H_{st}}{H_1}\right)}.$$

In the case of δ function (7) we get the following expression for Γ_δ by using the new variables (9):

$$\begin{aligned}\Gamma_\delta &= \frac{\pi e^2 n_h W_*^{1/2}}{\sqrt{2}cm^{1/2} W_0 N_w}\left(1-\frac{\omega_{H1}}{\omega}\right)\int_0^\infty \frac{\partial\left[\delta(W_* - Y)\right]}{\partial Y} \\ &\times \int_{X_{\min}}^\infty \left(\frac{H_{st}}{H_1}\right)^2 \frac{X \exp\left(-X/W_0\right)}{Y + X\left(1-\frac{H_{st}}{H_1}\right)}\, \mathcal{I}\, dX\, dY\end{aligned} \tag{11}$$

In the case of $z_{st} \neq 0$ we can use the simplified form for $\mathcal{I}$ [*Trakhtengerts et al.*, 1996],

$$\mathcal{I} = \frac{\pi a \cdot v_{\parallel st}}{2k(v_{\parallel L} - v_{RL})^{1/2}\left[\omega_{HL}/k + v_{\perp L}^2/(2\, v_{\parallel L})\right]^{1/2}} \tag{12}$$

where $a = \sqrt{2} R_0 L/3$ (R_0 is the Earth radius and L stands for L value for the dipole magnetic field). The value of z_{st} is equal to

$$\begin{aligned} z_{st} &= a\left(\frac{v_{\parallel L} - v_{RL}}{\omega_{HL}/k + v_0^2 H_L x/(2\, v_{\parallel L}\, H_1)}\right)^{1/2}, \\ & v_{\parallel L} - v_{RL} \geq 0 \end{aligned} \tag{13}$$

In (12) and (13) $v_{\parallel L}$ is the function of X and is equal to

$$v_{\parallel L} = \sqrt{v_*^2 + x v_0^2 \frac{\Delta H}{H_1}}$$

where $\Delta H = H_1 - H_L$. The values of $x_{\min}$ in (10) and $X_{\min}$ in (11) are determined from the following relations:

$$\begin{aligned} &\sqrt{v_*^2 + x_{\min} v_0^2 \tfrac{\Delta H}{H_1}} = v_{RL}, \quad \text{if } v_{RL} > v_* \\ &x_{\min} = 0 \qquad\qquad\qquad\quad \text{if } v_{RL} \leq v_* \end{aligned} \tag{14}$$

Substituting (12) into (11), we get

$$\begin{aligned}\Gamma_\delta &= -\frac{\pi}{4}\frac{\pi n_h e^2}{m}\frac{v_* v_0^2}{c^2}\frac{a\,(\omega_{H1} - \omega)}{k\,(k\omega_{HL})^{1/2}} \\ &\times \int_{x_{\min}}^\infty \left(\frac{H_{st}}{H_1}\right)^2 \frac{x \exp(-x)\, dx}{v_{\parallel st} \cdot v_{\parallel L}\,\left(v_{\parallel L} - v_{RL}\right)^{3/2}} \\ &\times \left(1 + \frac{k v_0^2 H_L}{2\, v_{\parallel L}\omega_{HL} H_1}\, x\right)^{-1/2}\end{aligned} \tag{15}$$

In the case of ΔH$\rightarrow$0 (the equatorial injection) the parallel velocity of the particles at the equator is v_*. The amplification Γ_{step} for the step from (10) is positive and singular as $(v_{\parallel L} - v_{RL})^{-1/2}$. So the Γ_{step} for particles whose equatorial parallel velocity coincides with the minimum parallel cyclotron resonance velocity goes to infinity as a result of the simple consideration in terms of (12), while only damping can be expected for the δ function in the simple consideration (15) and is singular as $(v_{\parallel L} - v_{RL})^{-3/2}$. Only the contribution for the amplification from the particles taking the energy from the wave is revealed. For the step as well as for the δ function, injection out of the equator ($\Delta H \neq 0$) puts some dispersion over x, meaning that the particle parallel velocity varies in accordance with the perpendicular velocity at the equator. This dispersion removes the singularity in the case of the step-like function but not in the case of the δ function. Apparently, the more strict consideration is required in the case $\Delta H \rightarrow 0$ and for the δ function by taking a more precise form of the phase mismatching of the cyclotron resonance condition Δ, which is given in the next two sections, 3 and 4.

3. The Case of Step-like Distribution (Strict Consideration)

As is shown in (10), one-hop amplification for the step function has a singularity in the case of ΔH$\rightarrow$ 0, which arises from the term $(v_{\parallel L} - v_{RL})^{-1/2}$ in $\mathcal{I}$(12). Here we pay much more careful attention to (3) instead of using (12) to evaluate the wave amplification. We take the Taylor series for the function $\Delta(z)$ near the stationary point z_{st} to estimate $\mathcal{I}$, and we get

$$\mathcal{I} = 4\left|\int_0^l dz \cos\left[\frac{\beta}{a^3}\left(\frac{z^3}{3} - z_{st}^2 z\right)\right] dz\right|^2 \tag{16}$$

where

$$\beta = \frac{\omega_{HL} a}{v_{\parallel st}}\left(1 + \frac{k v_0^2 H_L}{2 v_{\parallel L}\omega_{HL} H_1} x\right) \tag{17}$$

Equation (16) can be rewritten in the simple form by using the Airy function $Ai(-P)$ as follows:

$$\mathcal{I} = 4\pi^2 a^2 \beta^{-2/3} Ai^2\left[-P(x)\right] \tag{18}$$

where

$$P(x) = \beta^{2/3}\,(z_{st}/a)^2 = (ka)^{2/3}\frac{v_{\|L} - v_{RL}}{\left\{v_{\|st}^2\left(\frac{\omega_{HL}}{k} + \frac{v_0^2 H_L}{2v_{\|L}H_1}x\right)\right\}^{1/3}} \quad (19)$$

Now we can rewrite (10), using (17) and (18):

$$\Gamma_{\rm step} = \pi^{3/2}\frac{2\pi e^2}{m}n_h\frac{a^2}{v_0 c}\frac{\omega_{H1}-\omega}{\omega}\exp(-v_*^2/v_0^2) \times \int_{x_{\rm min}}^{\infty} x^2 e^{-x}\frac{H_{st}^2}{H_1^2}\frac{Ai^2[-P(x)]}{N_w\beta^{2/3}(v_{\|st}/v_0)^2}\,dx \quad (20)$$

This form can be used even under the condition $\Delta H \to 0$ and/or $v_{RL} = v_{\|L}$. Note that equations (16) and (18) for the interaction efficiency factor $\mathcal{I}$ take into account the existence of two resonance points symmetrically placed at both sides of the equator. The value of $\mathcal{I}$ depends on the electron-wave phase difference between these points, which is evidently a function of the electron parallel and perpendicular velocities and wave frequency. This is the cause of the oscillatory dependence of $\mathcal{I}$ on $P(x)$, which results in oscillations of the amplification as dependent on $v_* - v_{RL}$ or ω (see below).

We carried out the numerical computation of (20). We reduce the exact form (20) to a simplified one under several realistic conditions. First, the injection point and the stationary point z_{st} are located near the equatorial region, and hence $H_1 \simeq H_{st} \simeq H_L$ and $v_{\|st} \simeq v_* \simeq v_{\|L}$. Second, we consider the fixed wave frequency around $\omega \simeq \omega_{HL}/2$ instead of varying v_* as a free parameter. Third, we assume the cold plasma density n_c=7 cm^{-3} and a=1.74×10^4 km for $L = 6$. Finally, we suppose the characteristic velocity $v_0 \simeq v_*$. If $(v_* - v_{RL})/v_{RL} \ll 1$, then

$$(v_* - v_{RL})/v_{RL} \simeq (v_* - v_{RL})/v_* = (\omega - \omega_*)/\omega_* \quad (21)$$

where $\omega_* \equiv \omega_{HL} - kv_*$ is the angular frequency when the equality $v_{RL} = v_*$ is fulfilled. Now we shall move on to the computational results. Figure 1 shows the one-hop amplification versus $(ka)^{2/3}(v_* - v_{RL})/v_{RL}$ at three different injection points ($\Delta H/H_1$ = 0.0, 0.005 and 0.01). First, in the case of the injection point exactly at the equator ($\Delta H = 0.0$) the variation shows a sharp peak in growth near $v_{RL} = v_*$ coinciding with the stationary point being located near the equator followed by an oscillating tail. But it turns into a smooth decrease gradually when $(ka)^{2/3}(v_* - v_{RL})/v_{RL} \gg 1$. In the range of the smooth decrease the variation is well fitted by $(v_* - v_{RL})^{-1/2}$ in accordance with approximate formulas obtained for the one-hop amplification in the previous section by using (10) and (12). Amplitude of the oscillating tail decreases with increasing $(v_* - v_{RL})/v_{RL}$ (or increasing ω); however, the sign of the growth is positive over all the range considered. When the injection point is slightly away from the equator but still in the equatorial region ($0 < \Delta H/H_1 < 1$), the maximum growth points shift toward smaller values in $(v_* - v_{RL})/v_{RL}$ (lower-frequency range), and those peak values drop drastically when the injection point is getting away from the equator. In addition the sharpness of the peaks decreases when $\Delta H/H_1$ increases. The oscillating tail shifts toward larger $(v_* - v_{RL})/v_{RL}$ with the increase in $\Delta H/H_1$ and produces an isolated packet-like oscillation, which is seen significantly in the case of $\Delta H/H_1$=0.01.

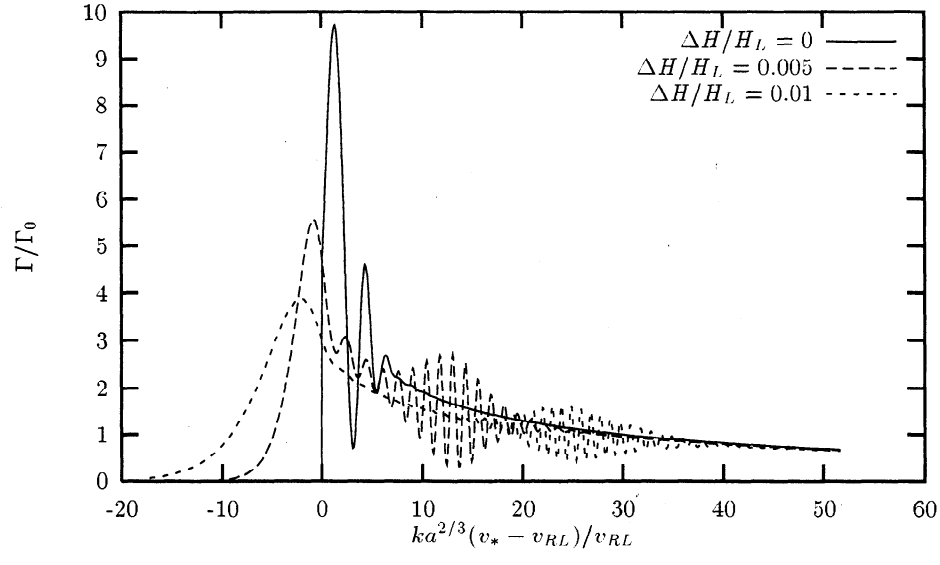

Figure 1. One-hop cyclotron amplification with the step-like distribution localized at different points relative to the magnetic equator. Amplification has been normalized to the maximum possible value for a smooth distribution with anisotropy $T_\perp/T_\| - 1 = 1$, $\Gamma_0 = 0.2(\pi/2)^{1/2}(n_h/n_c)(a/v_0)\omega_{HL}$. Plasma parameters are chosen as follows: $L = 6$, $n_c = 7$ cm^{-3}, $W_0 = 1.84$ keV(the latter corresponds to the condition $v_0 = v_{RL}$), and $\omega = 0.5\omega_{HL}$. For these parameters, $(ka)^{2/3} \simeq 431.5$.

Figure 2 shows the relation between the injection point $\Delta H/H_L$ and one-hop growth for different values of $(v_* - v_{RL})/v_{RL}$ (0.0, 0.003 and 0.005) near the first peak. In the case of $v_* = v_{RL}$ the maximum growth point is slightly away from the equator around $\Delta H/H_1 \simeq 0.002$. When $(v_* - v_{RL})/v_{RL}$ increases, the maximum point moves toward the smaller $\Delta H/H_1$ with increasing peak value and has a global maximum at a certain combination of $\Delta H/H_1$ and $(v_* - v_{RL})/v_{RL}$.

The above mentioned peculiarities can be explained in terms of the dispersive characteristics of the function $P(x)$. Originally, $P(x)$ in (19) is a product of the inhomogeneity factor β and the stationary point z_{st}/a, and x represents the perpendicular energy of the energetic particles.

Figure 3 shows the x dependence of $P(x)$ in several different combinations of $\Delta H/H_1$ and $(v_* - v_{RL})/v_{RL}$. First, we consider the case of equatorial injection (cases 1-(a) and 1-(b), $(v_* - v_{RL})/v_{RL}$ =0.003 and 0.07, respectively, under ΔH=0). $P(x)$ decreases smoothly with increasing x ($P(x) \propto x^{-1/3}$) for arbitrary $v_{RL}/v*$, and $P(0)$ increases with increasing $(v_* - v_{RL})/v_{RL}$. As is shown in curve 1-(a) (starting from $v_{RL} \simeq v_*$ (x_{min}=0)), $P(x)$ is nearly constant over the effective x range for the integration ($x \sim 2$) determined by the $x^2 \exp(-x)$ term, and $Ai(P(x))$ exibits a small dependence in x as well. Accordingly, the square of the Airy function, which has a first peak at $P(x) = 1.0$, is simply the function of $(ka)^{2/3}(v_* - v_{RL})/v_{RL}$ until one or two periods of the oscillation in Ai^2. On the contrary, starting from larger P(0) due to larger $(v_* - v_{RL})/v_{RL}$ (see the variation 1-(b)), the corresponding oscillation period of the Airy function is smaller, and the phase difference of Ai^2 within the effective integral range cannot be neglected anymore. As a result the net value integrated over x is suppressed as a results of incoherent summation in phase of Ai^2, which would diminish mainly the oscillation fringe. In addition to this effect, decreasing the amplitude of the Ai^2 in larger P also contributes to smaller amplification in larger $(v_* - v_{RL})/v_{RL}$. When the injection point is located away from the equator, $P(x)$ has a local minimum whose x value $x = x_M$ increases with decreasing $\Delta H/H_1$ and decreases with increasing $(v_* - v_{RL})/v_{RL}$. Examples are shown in curves 2-(a)-1, 2 and 2-(b)-1,2. In the case of $(ka)^{2/3}(v_* - v_{RL})/v_{RL}$ $\sim$1, $\partial P(x)/\partial x > 0$ around $x \sim 2$, and this gradient increases with increasing $\Delta H/H_1$ (see curves 2-(a)-1 and 2, $\Delta H/H_1$ = 0.003 and 0.01, respectively, under the same $(v_* - v_{RL})/v_{RL}$ =0.003). Accordingly, the average effect over x by the integration is significant, and the peak width would become larger. Also, $(v_* - v_{RL})/v_{RL}$ at the peak is getting smaller in larger $\Delta H/H_1$ as a result of the condition of the first peak in Ai^2 represented by the equality $P(x) = 1.0$. Meanwhile, the larger $(v_* - v_{RL})/v_{RL}$ becomes, the more the local minimum of $P(x)$ plays an important role in the behavior of the packet-like oscillation (see curves 2-(b)-1 and 2, $\Delta H/H_1$=0.003 and 0.01, respectively, under larger $(v_* - v_{RL})/v_{RL}$ =0.07). Around the points near the local minimum of $P(x)$: $x = x_M$, Ai^2 values are summed up coherently by integration over x, and the combination of $\Delta H/H_1$ and $(v_* - v_{RL})/v_{RL}$ under $x_M \sim 2$ would determine the peaks of the packet-like oscillating tail in $\Delta H/H_1$-$(v_* - v_{RL})/v_{RL}$ space. In fact, this relation is represented roughly as follows:

$$\frac{\Delta H}{H_1} \sim \frac{1}{8}\frac{v_* - v_{RL}}{v_*} \tag{22}$$

The curve 2-(b)-2 satisfies the above conditions, and generally, the peaks of the oscillating tail are well fitted by (22).

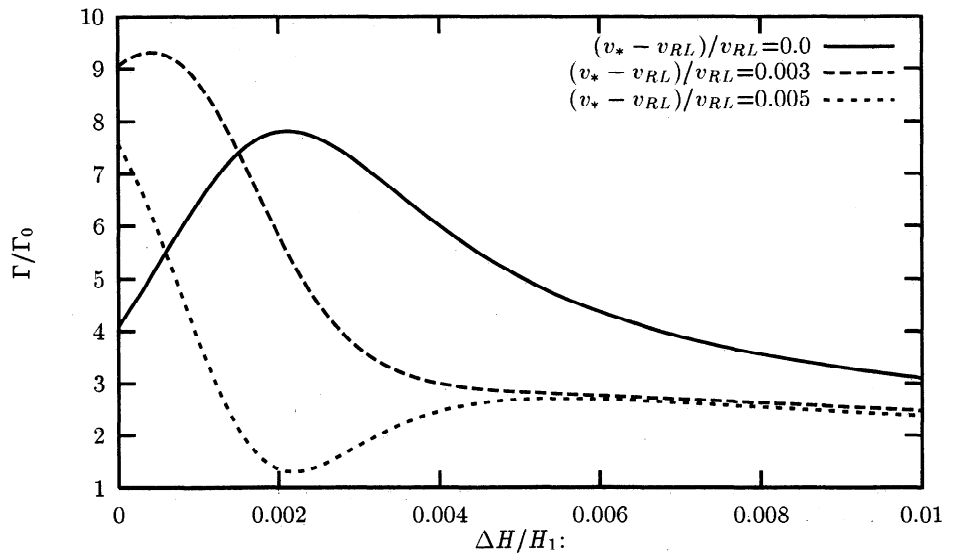

Figure 2. Dependencies of Γ on $\Delta H/H_L$ for different values of $(ka)^{2/3}(v_* - v_{RL})/v_{RL}$ near unity.

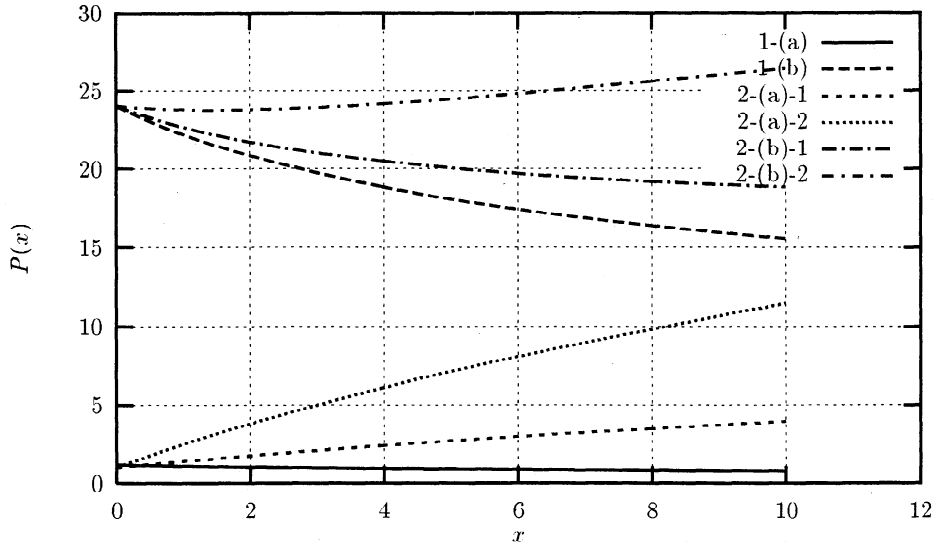

Figure 3. Dependence of $P(x)$ for different combinations of $\Delta H/H_1$ and $(v_* - v_{RL})/v_{RL}$. 1-(a) and 1-(b): ΔH=0 (equatorial injection) $(v_* - v_{RL})/v_{RL}$ =0.003 and 0.07 respectively; 2-(a)-1 and 2-(a)-2: $\Delta H/H_1 = 0.003$ and 0.01, respectively, under $(v_* - v_{RL})/v_{RL}$ =0.003; 2-(b)-1 and 2-(b)-2: $\Delta H/H_1 = 0.003$ and 0.01, respectively, under $(v_* - v_{RL})/v_{RL}$ =0.07.

4. Electron Beam with a Velocity Distribution of δ Function

In this section we consider the more strict approach for the amplification in the case of a δ function type distribution. Practically, we use the same approach as we have shown in the case of the step-like function in section 3. We can rewrite the form of the one-hop amplification for the δ function (11) with the Airy function and its derivative, using (18):

$$\Gamma_{\rm beam} = -\pi^2 \frac{4\pi e^2}{m} n_h \frac{a^2}{c^2} \left(\frac{W_*}{W_0}\right)^{1/2} \frac{\omega_{H1} - \omega}{\omega_{HL}} \times \int_{x_{L\,\min}}^{\infty} x e^{-x} \left(\frac{H_{st}}{H_1}\right)^2 \frac{Ai[-P(x)]\frac{dAi(-P)}{d(-P)}}{v_{\|L} v_{\|st}^2 / v_0^3} \times \frac{dx}{1 + k v_0^2 x/(2\omega_{HL} v_{\|L})} \quad (23)$$

The scale function $P(x)$ follows the definition in (19). We may use this form even in the case of ΔH$\rightarrow$ 0 and/or $(v_* - v_{RL})/v_{RL} \ll 1$.

Figure 4 shows the $(v_* - v_{RL})/v_{RL}$ dependence of one-hop amplification Γ for the two different injection points (one is at the equator and another is one away from the equator). A remarkable difference of this dependence from the step case is that Γ is sign alternative. In the case where the injection point is exactly at the equator, the sign of the amplification is positive at the point $(ka)^{2/3}(v_* - v_{RL})/v_{RL}$ =0.0. While $(ka)^{2/3}(v_* - v_{RL})/v_{RL}$ increases, the one-hop amplification increases and reaches the first peak at $(ka)^{2/3}(v_* - v_{RL})/v_{RL} \sim 0.5$ and the second peak at $(ka)^{2/3}(v_* - v_{RL})/v_{RL} \sim 3.0$ (largest among the peaks) after one of the biggest dampings. Then the oscillations in Γ continue at larger $(v_* - v_{RL})/v_{RL}$, but their amplitude decreases sharply with increasing $(v_* - v_{RL})/v_{RL}$.

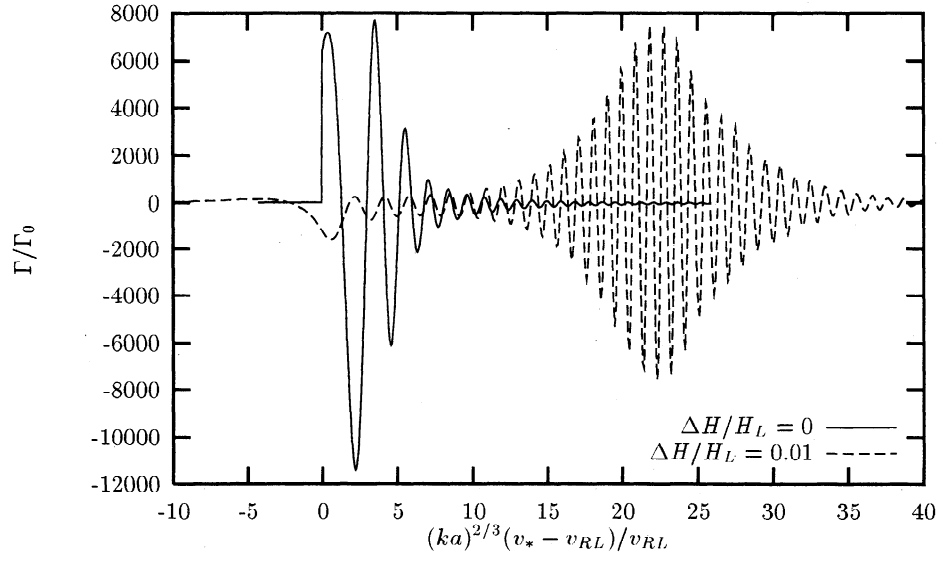

Figure 4. Same as Figure 1 but for the beam-like distribution in parallel velocity (7).

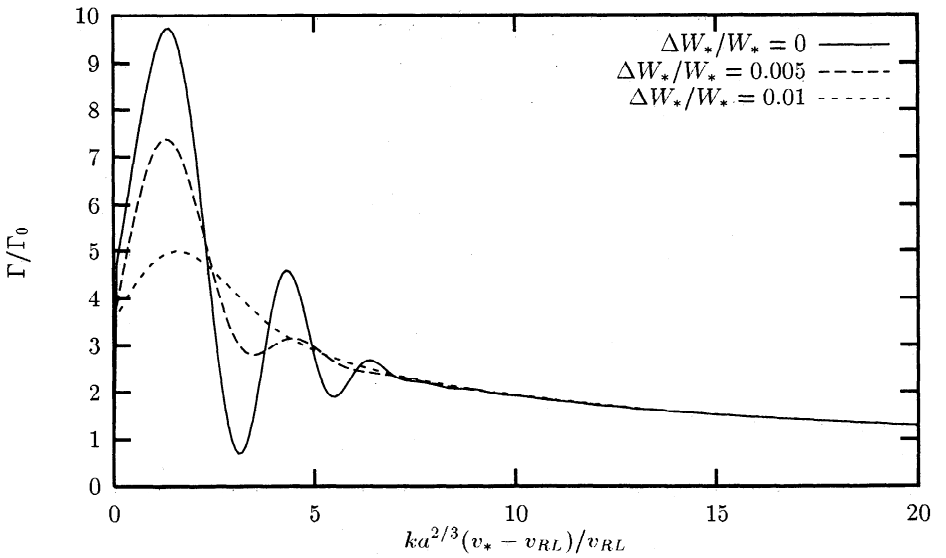

Figure 5. Influence of the parallel velocity dispersion on the one-hop cyclotron amplification with the step-like distribution localized at the magnetic equator. Plasma parameters chosen correspond to those in Figure 1.

One example in the case where the injection point is away from the equator ($\Delta H/H_1$ =0.01) is also shown in Figure 4. As can be seen, the positive peaks shift toward smaller $(v_* - v_{RL})/v_{RL}$, and the first peak has disappeared in larger $\Delta H/H_1$, but all the peak values drop significantly in comparison with the case of equatorial injection, and those peaks become broader. Note that the packet-like oscillating tail is also seen in larger $(v_* - v_{RL})/v_{RL}$, as is seen in the case of the step function. But an individual peak inside the tail is very sharp; the maximum amplitude within the peaks is about 3 times higher than that of the first peak and has either a positive or a negative sign. Practically, the characteristics of the variation shown in Figure 4 can be understood in the same manner as we studied in the case of step, meaning that the function $P(x)$ and the term including the Airy function integrated over x play the main role. However, the significant differences from the step case are that the term $Ai(-P) \times \partial Ai(-P)/\partial(-P)$ is the oscillating function having an alternative sign and that its amplitude is almost constant over P. Hence there is a much slower decrease in the amplitude of the oscillating tail in comparison with the step case in larger P, because only the average effect by integration over x would suppress the amplitude. Especially in the case of $\Delta H/H_1$ =0.01 the amplitude of the packet-like oscillation is comparable for the first and second peaks. The position

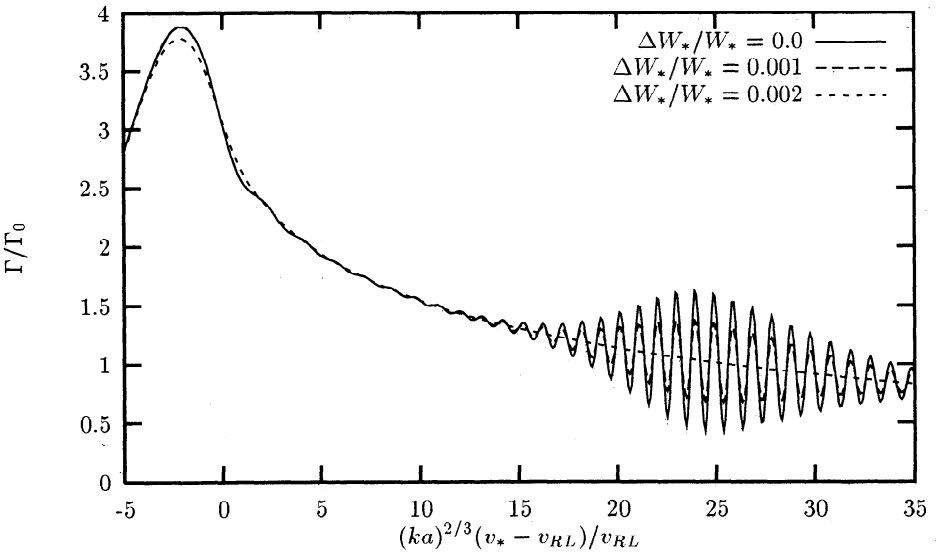

Figure 6. Influence of the parallel velocity dispersion on the one-hop cyclotron amplification with the step-like distribution localized away from the magnetic equator ($\Delta H/H_L = 0.01$). Plasma parameters chosen correspond to those in Figure 1.

of the peaks is well fitted by the function $\Delta H/H_1 \sim \frac{1}{7}(v_* - v_{RL})/v_{RL}$ derived by the derivative of $P(x)$ by x at $x \sim 1$, nearly similar in the case of step.

5. Effects of Small Dispersion in Parallel Velocity

Although formation of the distribution functions with step-like or δ-like features is theoretically predicted in space plasma conditions [*Karpman et al.*, 1974; *Nunn*, 1974; *Trakhtengerts et al.*, 1986, 1996], we do not know how sharp those gradients are. Thus it is worthwhile to investigate the influence of their smoothing over parallel velocity on the whistler wave amplification. From equations (10), (11), and (16)-(19) one can see that without the dispersion in $v_\parallel$ at the injection point the smallest scale in $v_\parallel$ in the integrands comes from the argument of the Airy function $P(x) \equiv \beta^{2/3}(z_{st}/a)^2$:

$$\Delta v_\parallel / v_\parallel \sim (ka)^{-2/3} \ll 1 \qquad (24)$$

Equation (24) determines which particles are almost synchronous with the wave at the stationary phase point z_{st}. Thus the idealized step-like or beam-like distribution, (5) or (7), respectively, will give the correct result for the amplification unless the dispersion in the parallel velocity does not exceed the value (24).

For the numerical calculations we used the following smooth approximation for the δ function:

$$\delta(Y - W_*) \approx \frac{1}{\pi^{1/2}\Delta W_\parallel} \exp\left[-\left(\frac{Y - W_*}{\Delta W_\parallel}\right)^2\right] \qquad (25)$$

Here, $\Delta W_\parallel = m v_\parallel \Delta v_\parallel$ is the dispersion in parallel energy. We substituted this representation into equation (10), for the step-like distribution, and into equation (11), for the beam-like distribution in parallel velocity, and performed numerical integration for different values of the parallel energy dispersion $\Delta W_\parallel$. Results of our calculations are shown in Figures 5–8. For the parameters chosen (see the caption in Figure 1), $(ka) \approx 430$; thus the idealized distributions (5) and (7) should provide correct amplitude values until

$$\Delta v_\parallel / v_\parallel = \Delta W_\parallel / 2W_\parallel \leq 2 \times 10^{-3}$$

This estimation is in good agreement with our numerical results.

6. Discussion and Conclusion

The calculations presented in the previous sections reveal some novel peculiarities of cyclotron wave-particle interactions in the case of well-organized distributions of energetic electrons. Analytical and numerical study has been performed on the basis of the third order expansion of the spatial dependence of the electron phase near the stationary phase point. For a step-like distribution the strict consideration provides a more complicated picture of the one-hop whistler wave amplification, in comparison with the earlier results [*Trakhtengerts et al.*, 1996; *Villalón and Burke*, 1997]. Cyclotron instability of the beam-like distribution in $v_\parallel$ in an inhomogeneous magnetic field has been considered for the first time. For both distributions we have investigated the effects of the finite dispersion in parallel velocity and the case when the sharp distribution is formed away from the equator.

The results obtained can be summarized as follows:

1. The one-hop whistler wave amplification is a sign-alternative function of the characteristic velocity v_* (or ω) for the beam-like distribution function (7), whereas it remains positive for the step-like distribution function

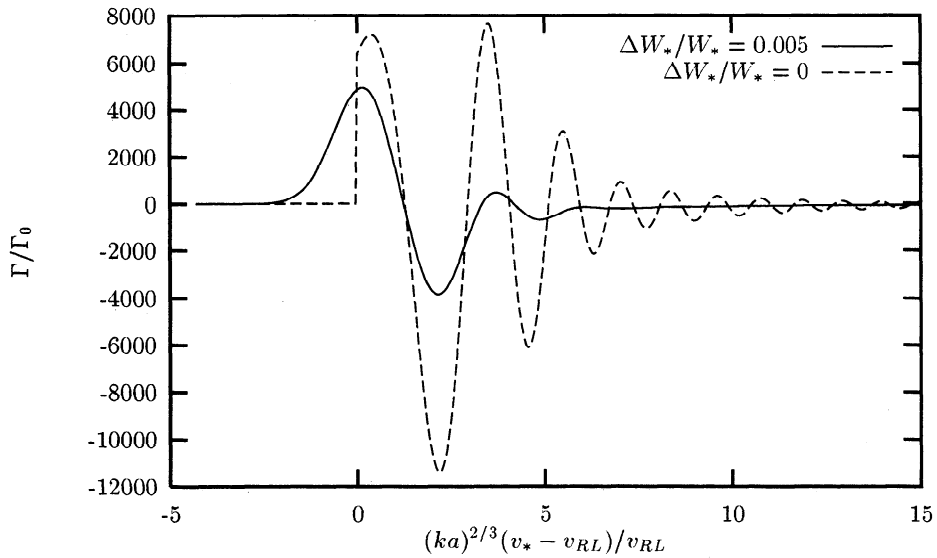

Figure 7. Influence of the parallel velocity dispersion on the one-hop cyclotron amplification with the beam-like distribution localized at the magnetic equator ($\Delta H/H_L = 0$). Plasma parameters chosen correspond to those in Figure 1.

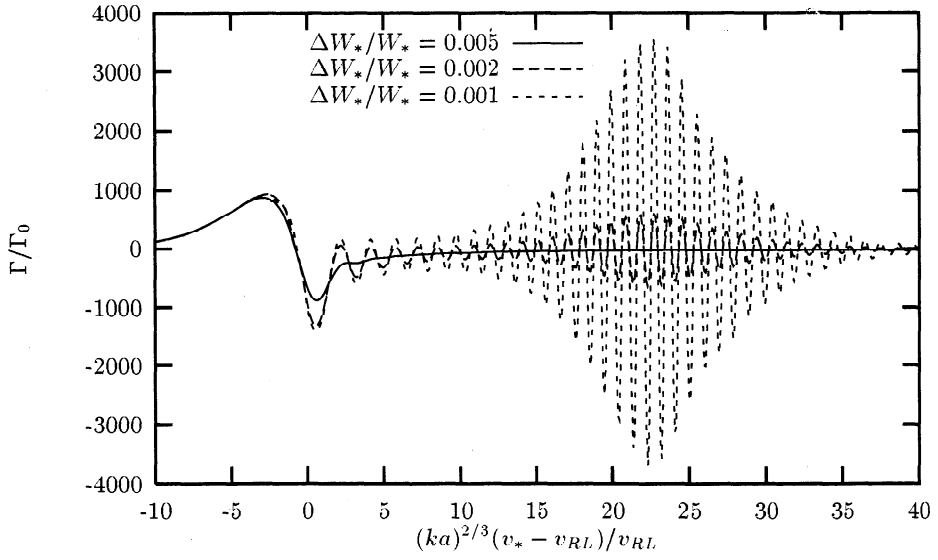

Figure 8. Influence of the parallel velocity dispersion on the one-hop cyclotron amplification with the beam-like distribution localized away from the magnetic equator ($\Delta H/H_L = 0.01$). Plasma parameters chosen correspond to those in Figure 1.

(5) (cf. Figures 1 and 4). The sign-alternative behavior for the beam could not be obtained with a simplified approach using the second order expansion of the electron phase spatial dependence (cf. sections 2 and 4).

2. The amplification Γ for step-like and beam-like distributions in $v_\parallel$ exhibits an oscillatory dependence on v_* (or ω); the characteristic frequency scale of oscillations is

$$\frac{\Delta\omega}{\omega} \sim \frac{\Delta v_{RL}}{v_{RL}} \sim \delta(ka)^{-2/3} \tag{26}$$

where the numerical coefficient $\delta \simeq 3$ for the first two maxima (Figures 1 and 4 8). Under the typical values $L \simeq 6$ and $\omega \approx \omega_{HL}/2$, $N_e \sim 7$ cm^{-3}, $\Delta\omega/\omega \sim 10^{-2}$, and $\Delta f = \Delta\omega/2\pi \sim 20$ Hz.

3. A packet-like oscillating tail appears in addition to the peaks in Γ near $(v_* - v_{RL})/v_{RL} = 0$ in the case of injection of the beam at a finite distance from the equator ($\Delta H \neq 0$, Figures 1 and 4). Near the exact resonance, $(v_* - v_{RL})/v_{RL} = 0$, Γ decreases with ΔH in both (step and δ) cases. However, Γ of the oscillating tail decreases in step case and grows in the δ case for small ΔH.

4. An increase of the dispersion $\Delta v_\parallel$ in the beam source leads to smoothing all oscillations and decrease of the peak growth rate; these effects become significant if the dispersion approaches and exceeds the value determined by equation (24) (see also Figures 5 8).

The discrepancy in sign of Γ for δ function between the simple and strict approach suggests the fact that careful consideration of the term $\mathcal{I}$, whose derivative in the parallel energy of particles determines the sign of the wave growth, is required. When the stationary point is located near the equator, the second term of the expansion in $\Delta(z)$ including $(\partial^2\Delta/\partial z^2)$ plays the main role in $\mathcal{I}$, as can be seen in (18), and gives rise to the oscillatory dependence as a function of z_{st} proportional to $(v_{\parallel L} - v_{RL})^{1/2}$ (i.e., that the relative contribution for the amplification from the particles giving their energy to the wave and taking the energy from the wave changes alternatively as a function of z_{st}), which would not be seen in (12). In other words, an inhomogeneity near the equator should be given precisely, making significant the effect in the variation of amplification. The oscillations in the amplification coefficient can give rise to narrow spectral peaks of whistler waves at the initial stage of instability; these peaks might serve as a seed for the sidebands seen in nonlinear computer simulations [e.g., *Nunn*, 1993]; however, the frequency separation between these nonlinear sidebands is controlled by the whistler wave amplitude, so there is no direct relationship between the peaks of the linear amplification and the sidebands.

For the δ function the amplification Γ is formally much greater than that for the step-like function with the same beam density: $\Gamma_\delta \sim (ka)^{2/3}\Gamma_{\rm step}$. However, in the real situation, when the beam as δ function is created by electron trapping in a quasi-monochromatic whistler wave packet [*Karpman et al.*, 1974; *Nunn*, 1974], its density n_b is much less than the full density n_h of the radiation belt electrons:

$$n_b \sim \frac{\Omega_{\rm tr}}{kv_R} n_h \sim \frac{(kv_{\perp 0}\omega_{HL}\, h)^{1/2}}{\omega_{HL} - \omega} n_h \tag{27}$$

where $h = b_L/H_L$ is the ratio of the wave magnetic field amplitude to the external magnetic field value and $\Omega_{\rm tr}$ is the trapping frequency of electrons. Taking, for example, $L = 6$, $kv_\perp/\omega \sim 1$, $\omega = \omega_{HL}/2$, and $b_L \sim 10$ mγ, we obtain $n_b/n_h \sim (2h)^{1/2} \sim 10^{-2}$.

Injection of the beam out of the equator leads to the velocity dispersion over $v_\parallel$, which appears in the pro-

cess of the beam expansion; this effect decreases the maximum value of Γ, but simplified estimations of Γ according to (11) and (15) are still not correct, and rigorous consideration, as in sections 3 and 4, is necessary. The δ distribution is more sensitive to the velocity dispersion than the step-like distribution. For example, if $\Delta H/H_L = 10^{-2}$ (this corresponds to the distance of the injection point from the equator $\Delta z \simeq 0.1a \sim 10^3$ km), Γ_δ decreases by a factor of 47 (Figure 4), and Γ_{step} increases only by a factor of 3 (Figure 1).

The sensitivity of the amplification to the resonance velocity, revealed in calculations (Figures 1 and 4), makes the second-order cyclotron resonance effects important. These effects appear in nonstationary formulation of the amplification problem and are not described by the basic formula (2). Thus the estimations of these effects made by *Villalón and Burke* [1997] in the framework of equation (2) seem to be not fully correct, and a more strict approach, taking into account nonstationary effects, is required. Such consideration is also important because, as a result of the very narrow amplification line in the case of well-organized distributions considered in this paper, the instability can become hydrodynamic under a rather small beam density. All these problems demand special consideration.

In summary, the results obtained indicate that amplification of narrowband emissions closely spaced in frequency is favored at the linear stage of the whistler cyclotron instability of the electron distribution functions with sharp features such as step or δ deformations, which are formed in the magnetosphere under electron-cyclotron interactions with noise-like emissions having upper frequency cutoff and quasi-monochromatic whistler signals, respectively. The characteristic frequency scale of these emissions in magnetospheric conditions has been found to be of the order of 20 Hz. The influence of the finite velocity dispersion on the amplification has been studied. The role of this initial stage of instability in the observed magnetospheric discrete emissions deserves future quantitative study in the framework of nonlinear analysis and simulations.

Acknowledgments. The work of V.T. and A.D. was supported in part by the Russian Foundation for Basic Research, grant 96-16473a.

The editor thanks Michael J. Rycroft and another referee for their assistance in evaluating this paper.

References

Bespalov, P. A., and V. Y. Trakhtengerts, The cyclotron instability in the Earth radiation belts, in *Reviews of Plasma Physics*, Vol. 10, edited by M. A. Leontovich, pp. 155–192, Plenum, New York, 1986.

Erokhin, N. S., N. N. Zolnikova, and L. A. Mikhailovskaya, On the gyroresonant interactions of electrons with a whistler in transition layers of the near Earth plasma, *Geomagn. Aeron.*, *36*(3), 84–91, 1996.

Hattori, K., M. Hayakawa, S. Shimakura, M. Parrot, and F. Lefeuvre, GEOS-I observations of hiss-triggered chorus emissions in the outer magnetosphere and their generation model, in *Proceedings of the NIPR Symposium on Upper Atmospheric Physics*, vol. 2, p. 84, National Inst. of Polar Res., Tokyo, 1989.

Hattori, K., M. Hayakawa, D. Lagoutte, M. Parrot, and F. Lefeuvre, Further evidence of triggering chorus emissions from wavelets in the hiss band, *Planet. Space Sci.*, *39*, 1465–1473, 1991.

Helliwell, R. A., A theory of discrete emissions from the magnetosphere, *J. Geophys. Res.*, *72*, 4773–4790, 1967.

Ivanov, A. A., *Physics of Strongly Nonequilibrium Plasmas* (in Russian), Energoatomizdat, Moscow, 1977.

Karpman, V. I., Y. N. Istomin, and D. R. Shklyar, Nonlinear theory of a quasimonochromatic whistler mode packet in inhomogeneous plasma, *Phys. Plasmas*, *16*(8), 685–703, 1974.

Nunn, D., A self-consistent theory of triggered VLF emissions, *Planet. Space Sci.*, *22*, 349–378, 1974.

Nunn, D., A novel technique for the numerical simulation of hot collision-free plasma: Vlasov hybrid simulation, *J. Comput. Phys.*, *108*(1), 180–196, 1993.

Nunn, D., and S. S. Sazhin, On the generation mechanism of hiss-triggered chorus, *Ann. Geophys.*, *9*, 603–613, 1991.

Trakhtengerts, V. Y., Magnetosphere cyclotron maser: Backward wave oscillator generation regime, *J. Geophys. Res.*, *100*(A9), 17,205–17,210, 1995.

Trakhtengerts, V. Y., V. R. Tagirov, and S. A. Chernous, Flow cyclotron maser and impulsive VLF emissions, *Geomagn. Aeron.*, *26*(1), 99–106, 1986.

Trakhtengerts, V. Y., M. J. Rycroft, and A. G. Demekhov, Interrelation of noise-like and discrete ELF/VLF emissions generated by cyclotron interactions, *J. Geophys. Res.*, *101*(A6), 13,293–13,303, 1996.

Villalón, E., and W. J. Burke, Theory of quasi-monochromatic whistler wave generation in the inner plasma sheet, *J. Geophys. Res.*, *102*(A7), 14,381–14,395, 1997.

A. G. Demekhov and V. Y. Trakhtengerts, Institute of Applied Physics, 46 Ulyanov Street, 603600 Nizhny Novgorod, Russia (e-mail: andrei@appl.sci-nnov.ru; vyt@appl.sci-nnov.ru)

M. Hayakawa and Y. Hobara, Department of Electronic Engineering, The University of Electro-Communications, 1-5-1, Chofugaoka, Chofu, 182-8585 Tokyo, Japan (e-mail: hayakawa@whistler.ee.uec.ac.jp; yasuhide@whistler.ee.uec.ac.jp)

(Received February 11, 1998; revised May 18, 1998; accepted May 19, 1998.)